Scientific Research Publishing

Journal of Materials Science and Chemical Engineering, 2022, 10, 30-43
https://www.scirp.org/journal/msce
ISSN Online: 2327-6053
ISSN Print: 2327-6045

Electrical Conductivity and Crystallization of Polylactic Acid Nanocomposites Containing Surfactant Modified Carbon Nanotubes

Qi Zhang*, Shijun Zhang

SINOPEC (Beijing) Research Institute of Chemical Industry Co. LTD., Beijing, China
Email: *zhangqi01.bjhy@sinopec.com

How to cite this paper: Zhang, Q. and Zhang, S.J. (2022) Electrical Conductivity and Crystallization of Polylactic Acid Nanocomposites Containing Surfactant Modified Carbon Nanotubes. *Journal of Materials Science and Chemical Engineering*, **10**, 30-43.
https://doi.org/10.4236/msce.2022.104003

Received: March 26, 2022
Accepted: April 26, 2022
Published: April 29, 2022

Abstract

In order to extend the usage of PLA-based nanocomposites, the modification of multi-walled carbon nanotubes (MWCNT) and preparation of surfactant modified carbon nanotubes (SMCNT) involved PLA nanocomposites (PLA/SMCNT) were investigated. The morphologies, electrical properties and crystallization behavior of PLA/SMCNT composites were investigated. The TEM images indicated that SMCNTs were dispersed homogenously in the PLA matrix without forming aggregates. The electrical conductivity of PLA/SMCNT was greatly improved and the percolation threshold of PLA/SMCNT was calculated to be 0.61% which is much lower than 1.45% of PLA/MWCNT composite. The crystallization behavior suggested that SDBS together with MWCNT acted as heterogeneous nucleating agent and accelerated the nucleation. Meanwhile, the SMCNT also devoted further restrained effect to spherulites growth due to its well dispersion and improved compatibility with matrix.

Keywords

PLA Nanocomposites, Carbon Nanotubes, Microstructures, Electrical Conductivity, Crystallization

1. Introduction

Polylactic acid (PLA) is renewable, sustainable, biodegradable, and eco-friendly thermoplastic polyester which is synthesized by the ring-opening polymerization of lactides and lactic acid monomers [1] [2] [3]. PLA has been widely researched and used in the areas of biomedicine, tissue engineering, packaging application, etc. because of its excellent biological performance and other attractive properties comparable with petroleum-based polyolefin [4] [5]. Although PLA has balanced properties of mechanical strength and thermal plasticity, the brittle nature and insulating property of pure PLA greatly limit its widespread acceptance. Yet, it is necessary to improve the electrical conductivity of PLA composites for some applications for which electrical charge mitigation is a key design constraint [6]. The method of functionalizing insulating polymers with electrically conductive nanoscale fillers is essential to ensure improved electrical conductivity in PLA.

Carbon nanotubes are one of these promising nanofillers and have received considerable attention by scientists since it firstly was reported by Iijima [7]. As known to all, carbon nanotubes possess high flexibility, low mass density, and large aspect ratio (typically > 1000), whereas they present extraordinarily high tensile strength and modulus, together with excellent electrical properties [8] [9] [10]. Undoubtedly, the combination of PLA with CNTs could impart electrically properties to the matrix and broaden the novel application in conductive polymer composites (CPC) and many other fields [11] [12]. However, the aggregation of carbon nanotubes in polymer composites is still the fundamental and technical barriers toward expanding many of the applications. Therefore, it is a critical point to make the efficient dispersion of individual CNT and establish a strong interaction with the matrix.

In the cases of PLA-based nanocomposites, the modification (covalent or noncovalent) of CNTs is the most commonly way to enhance the dispersion and interface bonding [13] [14] [15] [16]. Besides that, there are also some studies on the formation of conductive network in stereo-complex [17]. The CNT incorporated with poly L-lactic acid (PLLA) and poly D-lactic acid (PDLA) exhibited excellent electrical conductivity with a very low electrical percolation threshold [12] [18] [19], allowing an insulator turn into semi-conductive or conductive materials by creating a CNT network. So far, many researches showed that the dispersion of CNTs and the interfacial adhesion between phases can be improved by grafting functionalize of CNTs with PLA itself or polymers that have good compatibility with the matrix [20] [21]. The investigations also revealed that the chemical modification more or less caused structure damage of CNTs thus might have negative influence on the performance of electrical conducting. In contrast, the noncovalent modify routes are considered more promising since the electronic structure and properties of the CNTs can be better preserved [22].

In this study, sodium dodecyl benzene sulfonate (SDBS) was utilized to noncovalent modify the carbon nanotubes. The effects of surfactant modification on the dispersion of CNTs and the performances of PLA-based nanocomposite on electrical conducting and crystallization were detailed investigated. SMCNT is a shortened form of surfactant modification carbon nanotubes. The surfactant SDBS is quite ideal to modify the MWCNTs, not only because the process generated interaction altered the aggregated state of MWCNTs, but also the long alkyl chains in SDBS molecules that can wrap the tubes make the filler compatible with PLA matrix [23]. With the SDBS non-covalent modification, the dispersion of MWCNTs is significantly improved. The well dispersion of fillers resulted in the greatly improved conductive capability. The addition of only 1 wt% carbon nanotubes in the composites increased the electrical conductivity from 10^{-17} to 10^{-8} S·cm. In contrast, the addition of MWCNT without the surfactant only had moderate effect on the enhancement of electrical properties.

2. Experiment

2.1. Materials

The MWCNTs (>98%, with an outside diameter of 20 - 30 nm, an inside diameter of 5 - 10 nm, and lengths of 10 - 30 μm) were purchased from Cheap tubes Co., Ltd, USA, and used as received. The PLA (3051D) was provided by Nature Works, USA, with the following characteristics: specific gravity 1.24 g/cm^3, melt index 10 - 25 g/10min (190˚C), melting temperature 150˚C, glass transition temperature (T_g) 61˚C, average molecular weight (Mw) 90,000 - 120,000, optical purity of 96 wt.%. Sodium dodecyl benzene sulfonate (SDBS) (purity > 99%) was purchase from Aldrich and used without further purification.

2.2. SDBS Modification and Nanocomposite Processing

Anionic surfactant, sodium dodecyl benzene sulfonate (SDBS), with different concentrations was used to modifying MWCNTs. The MWCNTs were added to the surfactant solutions by varied weight ratio of SDBS/MWCNT. Then, the mixture was ultrasonicated at room temperature for 1 h. The resulted suspensions were then centrifuged for 20 min at 10,000 rpm to remove the precipitates and bundles.

The PLA-based nanocomposites were prepared by Haake MiniLab. All the materials were pre-dried overnight before extraction in vacuum at 60˚C to remove eventual traces of moisture. PLA were dried in vacuum oven at 80˚C for 6 - 8 h, and then the PLA/SMCNT composites with a MWCNT weight ratio of 0.5% - 3% as well as pure PLA/MWCNT composites were extruded by Haake Twin-screw at 190˚C. The real temperature of each screw section is 175˚C, 185˚C, 190˚C, 190˚C, 190˚C, and 180˚C.

2.3. Electrical Properties

The samples were compression molded into round slices with diameter of 10 cm and thickness of 1 mm. The volume resistance of the samples was measured by a PC6 8 digital tera ohmmeter, and then volume electrical conductivity was calculated.

2.4. Morphology Observation

The morphology of PLA/MWCNT and PLA/SMCNT composites was examined by transmission electron microscopy (TEM) using a FEI Tecnai-20 instrument, the samples were prepared through frozen section.

2.5. Thermal Analysis

The thermal behavior of composites was studied by differential scanning calorimetry (DSC, PerkinElmer Diamond) under nitrogen atmosphere. The samples (ca. 5 - 8 mg) were heated to 230˚C and held for 5 min to eliminate thermal history in the materials and then cooled to 0˚C at a rate of 5˚C/min. At last the samples were reheated to 230˚C at a rate of 5˚C/min.

2.6. Isothermal Crystallization

The isothermal crystallization was performed on an optical polarizing microscope (POM, Olympus BX51TF model, Japan) with a Cool snap Color3.3M digital camera and a Linkam hot-stage. The crystallization temperatures were chosen at 120˚C. All samples were heated to 210˚C and held for 5 min to eliminate any thermal history in the materials and then rapidly cooled to 120˚C, keeping a certain time for isothermal crystallization.

3. Results and Discussion

3.1. Effect of SDBS Concentration on the CNTs

As known to all, MWCNTs had tendency to agglomerate and bundle together because of strong forces originated from physical entanglements and high Van Der Waals forces between neighboring tubes, limited the efficiency of MWCNT in the nanocomposite. Generally speaking, the dispersion states of MWCNTs directly decide the interaction with matrix and the formed conductive network structures which provide transfer path for electrons [24]. The MWCNTs formed aggregates suggest less efficiency use of MWCNT properties. As shown in **Figure 1**, the pristine MWCNTs (**Figure 1(a)**) mostly presented curly and aggregated state with about 15 - 30 nm diameters. After SDBS modification, the SMCNT showed extended state and decreased aggregation. We can easily find mono-dispersed MWCNTs in **Figure 1(b)**. Moreover, we measured average diameters of MWCNTs and SMCNTs from SEM and the results proved that the apparent diameters of SMCNT could be adjusted by changing the weight ratio of surfactant SDBS and MWCNTs (**Figure 1(c)**). The SEM also gave us an indication that by modification the MWCNTs were well coated by a thin SDBS layer.

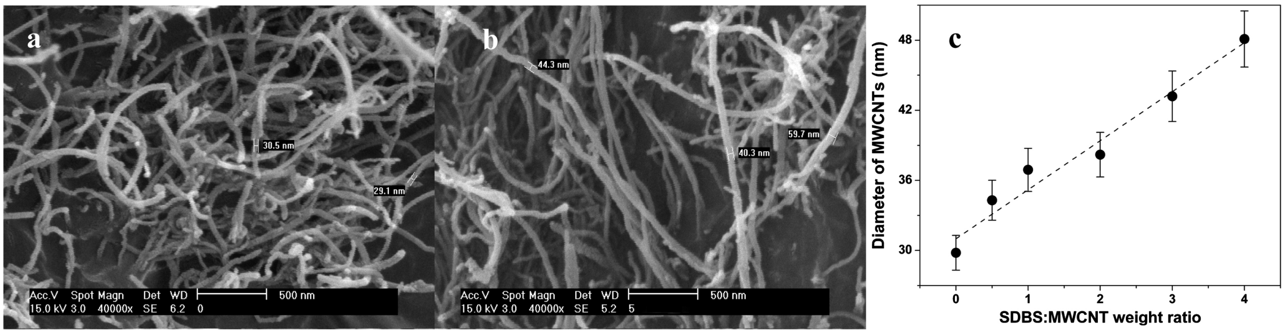

Figure 1. SEM images of MWCNT (a) and SMCNT (b), The weight ratio of SDBS/MWCNT is 1 for (b). The effect of (SDBS: MWCNT) weight ratio on the diameter of MWCNTs (c).

The good coating of surfactant can be explained by strong π-π stacking interactions between the outer surfaces of the MWCNTs and the phenyl rings on SDBS. Long-chain alkyl segments in SDBS played an important role in wrapping MWCNTs [6].

3.2. Dispersion of SMCNT in the PLA/SMCNT Nanocomposite

In order to better understand PLA/SMCNT composites, the morphologies of composite samples are investigated by SEM and TEM (**Figure 2**). The difference between the PLA/MWCNT and PLA/SMCNT composites was clearly represented in **Figure 2**, typically the pristine MWCNTs appeared to be curly and mostly aggregated which are indicated by red arrows in **Figure 2(a1)**. The dispersion state of pure MWCNTs suggests the interaction between the CNT and PLA matrix was not so good. Meanwhile, a well dispersion with no obvious agglomerations of SMCNT can be observed in **Figure 2(b1)**, **Figure 2(b2)**, **Figure 2(b3)**. The PLA/SMCNT sample seems have rougher fraction surface which also indicated the improvement of affinity between fillers and matrix. The crack in the cross section (**Figure 2(b1)**) might cause by high electrical energy during the SEM scan.

The dispersion and state of MWCNT in the fractured composites samples can be easily distinguished with higher magnification. The TEM morphology suggested the agglomerated state of MWCNTs and revealed its weak interactions with PLA matrix (**Figure 2(a2)**, **Figure 2(a3)**). Most MWCNTs were bundled and agglomerated at the same content of 1%, the aggregates of SMCNT barely can be found and the carbon nanotubes were distributed in a

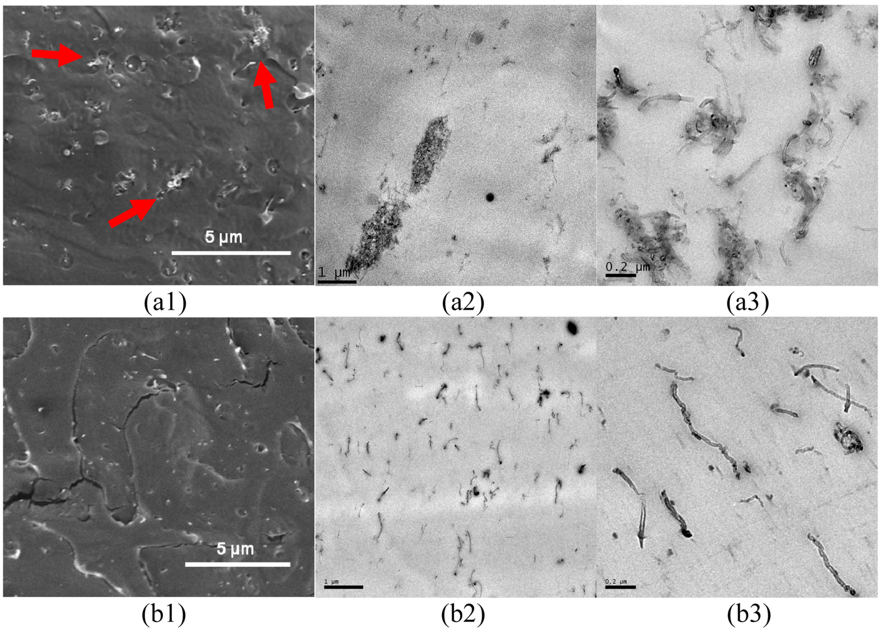

Figure 2. The SEM and TEM of PLA/MWCNT (a1)-(a3) and PLA/SMCNT (b1)-(b3) composites, the CNT loading of composites is 1 wt.%. Clearly, the pure MWCNT is observed agglomerated while the SMCNT presented separately dispersion.

kind of elongate state (**Figure 2(b2)**, **Figure 2(b3)**). It can be observed that the SMCNTs in the fractured samples with different CNT loading contents (0.5% - 3.0%) are evenly distributed and approximately aligned along one direction. The observations indicated that the SDBS modification process could greatly improve the MWCNT dispersion thus facilitate the formation of the conductive network with a relatively low MWCNT concentration.

3.3. The Optimum of [SDBS/MWNTs] Ratio

Non-covalent modification of SDBS on the surface of MWCNT can improve the combination of carbon nanotubes with polymer and facilitate the dispersion of CNTs in the matrix. The SDBS concentration used in modification decided the formation of cladding layer around MWCNT and its thickness which might have effect on the electron transmission. Thus, we investigated the effect of varied SDBS concentration on the conductive capability of PLA/SMCNT nanocomposite. The volume resistivity of PLA/SMCNT composites which contained MWCNT that modified by varied concentration of SDBS was shown in **Figure 3**. Apparently, the variation tendency of electrical conductivities was relevant with the SDBS concentrations. In the certain weight ratio of 0 - 1, the volume resistivity continually decreased and appeared a minimum value at the ratio of 1. After that, the increasing SDBS concentration leads to the elevation of electrical resistivity.

Alig [25] have established a relation between state of CNT dispersion, structure of the CNT network and electrical properties, proposing that small CNT-CNT distance facilitate the formation of a network of dispersed agglomerated CNT for the electrical conducting. This theory could clearly explain

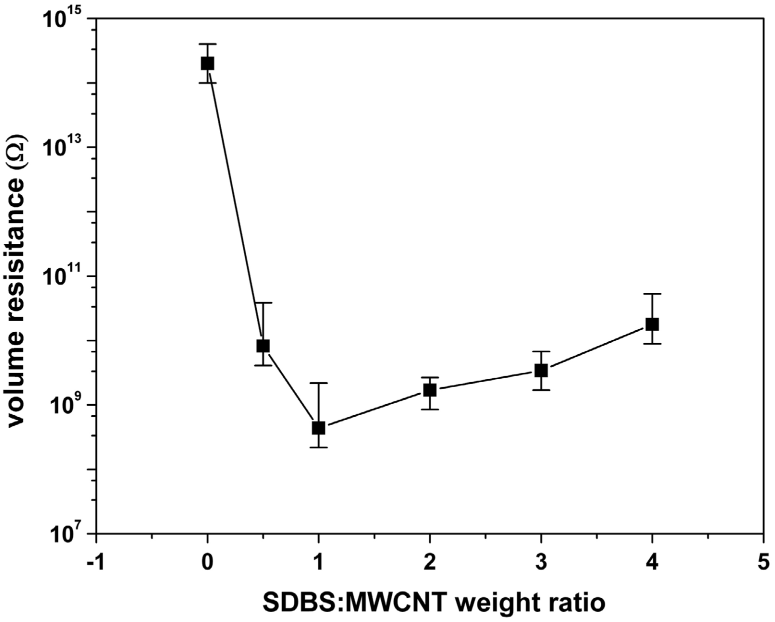

Figure 3. The effect of reactant ratio (SDBS/MWNTs) on the volume resistance of PLA/SMCNT composite.

the effect of SDBS amount on the composite's electrical properties. The role of SDBS is mainly to function as a dispersing agent. The SDBS interacted with MWCNT through the hydrophilic segment and the formed layer could provide a steric repulsive force which overcomes the Vander Waals attractive force between the MWCNT surfaces [26]. The added amount of SDBS directly affected the CNT-CNT distance. With too much SDBS amount, the generated steric repulsive force might prevent the formation of conductive network. A proper addition could the CNTs dispersed homogeneously and maintain a closely distance of CNT-CNT ensuring to get connection and transfer electrons. Therefore, an optimum [SDBS/MWCNT] ratio amount is chosen to provide proper interaction force which could alter seriously CNT aggregation status without making CNTs separately and disconnect.

3.4. Electrical Conductivity of PLA/SMCNT Nanocomposites

In order to further investigated the electrical conductivity of PLA/SMCNT nanocomposites, we prepared a series of PLA/SMCNT nanocomposites with SMCNTs that modified by varied SDBS concentrations. **Figure 4** presents the effect of MWCNT loading with and without SDBS modification on the electrical conductivity of the nanocomposite with specific values. As shown in **Figure 4**, the conductivity of pure PLA is below 10^{-16} S/cm which illustrated the conductive mechanism of PLA/MWCNT composites refers to the electron transfer in the path of MWCNTs [12]. For PLA/MWCNT, the volume electrical conductivity maintains a value about 10 - 15 S/cm when the percentage of MWCNTs is below 1%. That revealed the MWCNTs without any treatment cannot form an efficient bridged linkage in PLA matrix at lower loading range. It can be observed that, different from PLA/MWCNT composites, the volume electrical conductivity of PLA/SMCNT (**Figure 4(a)**) presented sharply enhancement with the increasing SMCNT content even at low CNT loading. The electrical conductivities of PLA/SMCNT composites exhibit a typical percolation behavior with an increase order of 8 - 9 of magnitude close to 0.6 wt.% loading content which is 1.3% - 1.5% for PLA/MWCNT composites. This superior of SDBS modification to unmodified composite clearly distinguished from the curves in **Figure 4(a)** and **Figure 4(b)** indicated the conductive network formed with largely lower filler content. The standard deviation which can be observed near the weight fraction provided evidence for the percolation filler network and the pathway from an insulating to a semi-conductive material [18]. A scaling law relation (1) is used to determine the percolation threshold [27].

$$\sigma = \sigma_0 \cdot \left(\phi - \phi_c\right)_t \tag{1}$$

where σ and σ_0 are the electrical conductivity of the nanocomposites and the polymer matrix respectively (S/m), ϕ is the MWCNT mass fraction (wt.%), ϕ_c is the threshold of the electrical conductivity percolation and t is the critical exponent.

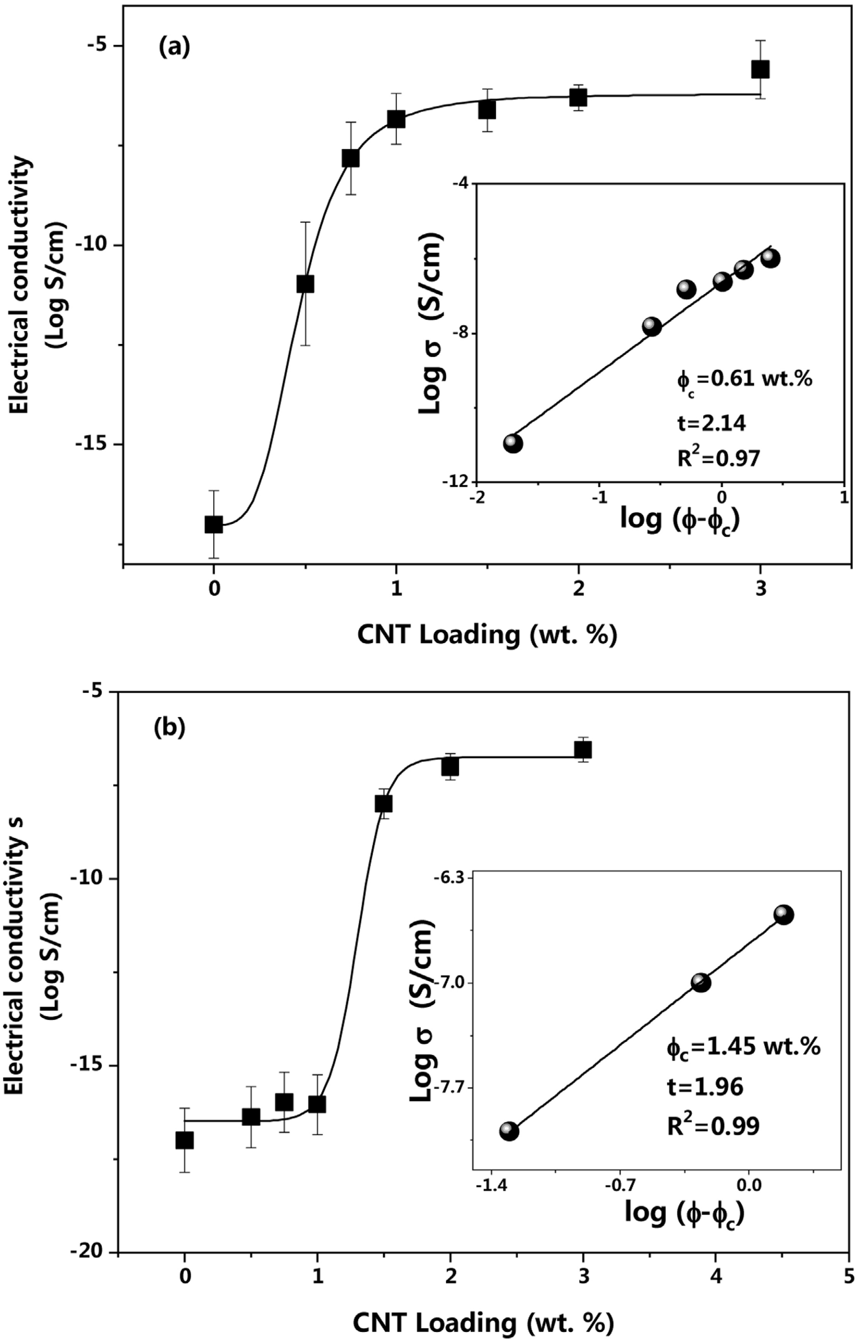

Figure 4. Effects of CNT contents on the electrical conductivity σ (S/cm) of PLA/SMCNT (a) and PLA/MWCNT (b) composites. The insert graphs represented the log-log plot for σ vs ($\phi - \phi_c$). Results of σ are fitted by incrementally varying ϕ_c until the best linear fit to equation was found.

Based on the percolation theory, the electrical percolation threshold decided the critical content of conductive fibers which required constructing the conductive networks. The curve fitted from Equation (1) gives ϕ_c = 0.61 wt.%/t = 2.14 and ϕ_c = 1.45 wt.%/t = 1.16 for PLA/SMCNT and PLA/MWCNT nanocomposite, respectively. The t values indicate for PLA/SMCNT composite a transport in three dimensions when the PLA/MWCNT in two dimensions [18]. The percolation threshold of the PLA/SMCNT composites is much lower than that of PLA/MWCNT composites when the differential is done. The relatively low percolation threshold is attributed to the homogeneous dispersion of SMCNT and optimal contact between CNT in the PLA matrices which were realized by SDBS modification process. Typically, 1 - 3 wt.% CNT loading is required to reach an electrical percolation threshold for nanocomposites produced by melt processing *i.e.* using extrusion/melt compounding [28]. Usually, the primary agglomerates of high cohesive strength make the uniform distribution of CNT in the viscous polymer much difficult. Our results clearly indicated the efficiency of SDBS modification can have on improving the electrical conduction of composites and gave useful information for dispersing CNT in PLA type of materials. The future studies involving different surfactant types and concentration for different polymer as well as more complete understanding of composite properties and the interfacial chemistry will be taken on.

3.5. Crystallization Behavior

Optical microscopy and differential scanning calorimetry (DSC) were used to figure out the effect of SDBS on the crystallization of MWNT/PLA nanocomposites. **Figure 5(a)** exhibits the perfect spherulites of PLA. As foreign matters, SMCNT which served as the nucleating agent altered the density and integrity of spherulites. Different from PLA, both PLA/MWCNT and PLA/SMCNT composites generated small and incomplete crystal. According to the isothermal crystallization results, the induction time of PLA nanocomposite which was observed as 10 min was reduced by introducing MWCNT and further decreased by surfactant modification process. The induction time of PLA/MWCNT and PLA/SMCNT presented to be 9 min and 7 min, respectively. It is easy to distinguish that more crystals were generated in PLA/MWCNT and PLA/SMCNT composites than that of PLA within the same crystallization time. That indicated the addition of MWCNT increases the nucleation density and speeds up the spherulites growth [22]. The generated incomplete spherulites (as we can see in **Figure 5(c)**) also suggested that the SDBS modification decrease the crystallization.

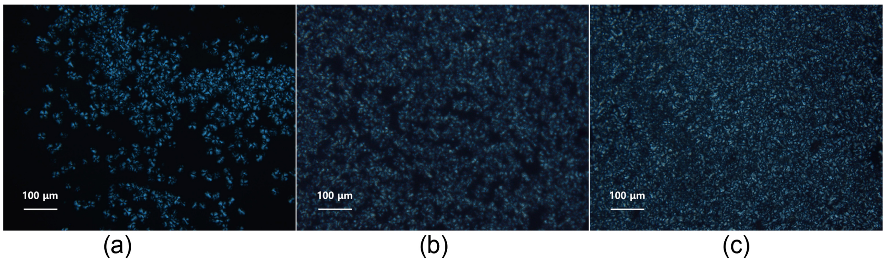

Figure 5. Polarization micrographs of pure PLA (a), PLA/MWCNT (1%) (b) and PLA/SMCNT (1%) (c) composites which isothermal crystallized at 120˚C for 20 min.

The DSC of samples was also measured to investigate the influence on the composites caused by the SDBS modification. All of the samples were heated to 230˚C at a rate of 5˚C/min after melt-quenching for monitoring the cold crystallization of the nanocomposites. The glass-transition temperature (T_g), the cold crystallization temperature (T_{cc}) and the melting temperature (T_m) of nanocomposites were analyzed and partial results were shown in **Figure 6**.

As we can see in **Figure 6(a)**, no obvious exothermic peak can be observed for

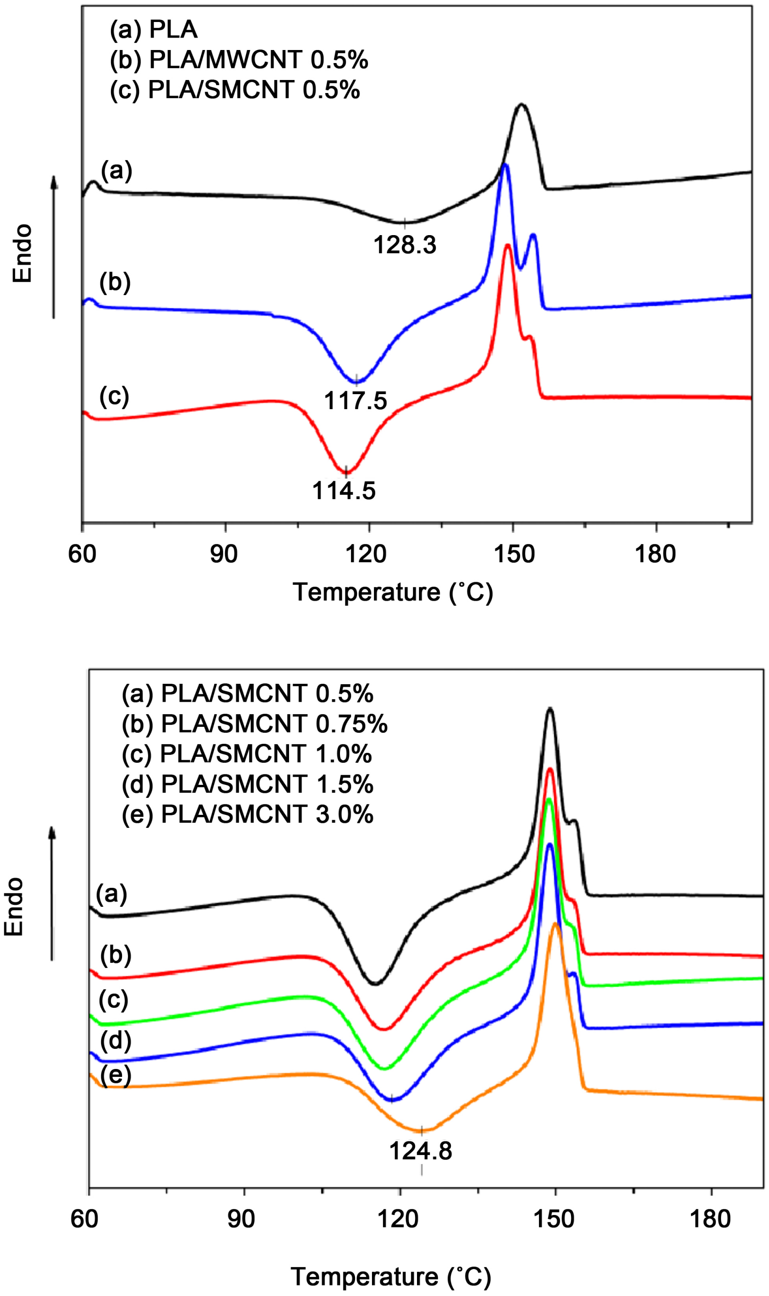

Figure 6. DSC curves of PLA/MWCNT and PLA/SMCNT composites, (a) comparison between PLA, PLA/MWCNT and PLA/SMCNT; (b) effect of CNT content on the melting of PLA composites.

pure PLA, and that is related to the low nucleation ability of PLA. In the subsequent heating step, a cold crystalline peak of composites became more evidently after blending with MWCNT and SMCNT fillers. Compared to PLA, clearly both PLA/MWCNT and PLA/SMCNT composites presented much distinguished cold crystallization peak and had decreased T_{cc} value. T_{cc} values of the PLA/MWCNT composite sample decreased from 128.3˚C to 117.5˚C, and even more for that of PLA/SMCNT composite (114.5˚C). The facilitation was undoubtedly due to the effect of MWCNT which acts as heterogeneous nucleating agent and accelerates nuclei generation [12]. The T_{cc} value of PLA/SMCNT composite, which is lower than that of PLA/MWCNT composite, indicated the enhanced nucleating function of SMCNT with SDBS coating. In addition, the molten peak of PLA split into a double and the T_m value decreased from 154˚C in PLA to 150˚C with no change afterward because of the addition of MWCNTs. The appearance of a doublet may due to recrystallization of incomplete spherulites. The SDBS existence further induced the generation of incomplete spherulites.

In **Figure 6(b)**, with the increasing content of SMCNT, the T_{cc} value shifted to higher temperature, reaching a value of 124.8˚C, and the split molten peak gradually became one integral peak when the SMCNT content is up to 3.0%. That result is not accord with that of MWCNT composites (without modification) which has been reported before [23]. We consider the phenomenon as a further restrained effect since SDBS modification may improve the dispersion of MWCNT and the compatibility between the filler and the matrix. According to the reference, unmodified MWCNT do not disperse well (no matter its content) and just serve as impurities without a further effect when the content increase [29]. Unlike MWCNT, SMCNT present well dispersion and possess a large aspect ratio (as we can observed in TEM images) thus could provide much more nuclei for spherulite growth as well as the restrained effect. Yet, at higher content of SMCNT, the generated nuclei could not obtain high crystallization because of the relative low growth rate and limited molecule space. The change of melt peaks of PLA/SMCNT composite with the increasing SMCNT content suggested the transition of crystal phase to imperfect.

4. Conclusion

PLA/SMCNT nanocomposites blending with SDBS modified MWCNT are prepared and compared with PLA/MWCNT. The morphologies of PLA/SMCNT nanocomposites indicated the SDBS layer improved the dispersion of MWCNTs in PLA matrix and facilitated the formation of conductive network thus enhanced the conducting capability of the composite. The electrical properties of PLA/SMCNT were greatly improved by comparing with PLA/MWCNT composites and the percolation threshold was reduced from 1.45 wt.% to 0.61 wt.%. The exponent value of $t = 2.14$ suggested for PLA/SMCNT composite a transport in three dimensions. The SDBS, together with MWCNTs, acted as nucleating agent and accelerated the crystallization process of composites. The cold crystallization temperature of PLA/SMCNT nanocomposites shifted to higher temperatures when the content of SMCNT increased. The results of our work clearly indicated the effect of SDBS modification for dispersing MWCNT in PLA matrix. Future improvement of this work may include a more complete understanding of composites properties and better choices of surfactant types as well as optimization of CNT contents in PLA matrix for different applications.

Acknowledgements

The authors declare no conflicts of interest regarding the publication of this paper.

Conflicts of Interest

The authors declare no conflicts of interest regarding the publication of this paper.

References

[1] Wang, F., Wang, G., Ning, F. and Zhang, Z. (2021) Fiber-Matrix Impregnation Behavior during Additive Manufacturing of Continuous Carbon Fiber Reinforced Polylactic Acid Composites. *Additive Manufacturing*, **37**, 101661-101672. https://doi.org/10.1016/j.addma.2020.101661

[2] Gürler, N., Paşa, S., Hakkı Alma, M. and Temel, H. (2020) The Fabrication of Bilayer Polylactic Acid Films from Cross-Linked Starch as Eco-Friendly Biodegradable Materials: Synthesis, Characterization, Mechanical and Physical Properties. *European Polymer Journal*, **127**, 109588-109596. https://doi.org/10.1016/j.eurpolymj.2020.109588

[3] Mokhena, T.C., Sefadi, J.S., Sadiku, E.R., John, M.J., Mochane, M.J. and Mtibe, A. (2018) Thermoplastic Processing of PLA/Cellulose Nanomaterials Composites. *Polymers* (*Basel*, *Switz.*), **10**, 1363-1391. https://doi.org/10.3390/polym10121363

[4] Siakeng, R., Jawaid, M., Ariffin, H., Sapuan, S.M., Asim, M. and Saba, N. (2019) Natural Fiber Reinforced Polylactic Acid Composites: A Review. *Polymer Composites*, **40**, 446-463. https://doi.org/10.1002/pc.24747

[5] Sangeetha, V.H., Deka, H., Varghese, T.O. and Nayak, S.K. (2018) State of the Art and Future Prospectives of Poly(lactic acid) Based Blends and Composites. *Polymer Composites*, **39**, 81-101. https://doi.org/10.1002/pc.23906

[6] Zhou, J. and Lubineau, G. (2013) Improving Electrical Conductivity in Polycarbonate Nanocomposites Using Highly Conductive PEDOT/PSS Coated MWCNTs. *ACS Applied Materials & Interfaces*, **5**, 6189-6200. https://doi.org/10.1021/am4011622

[7] Iijima, S. (1991) Helical Microtubules of Graphitic Carbon. *Nature*, **354**, 56-58. https://doi.org/10.1038/354056a0

[8] Rathinavel, S., Priyadharshini, K. and Panda, D. (2021) A Review on Carbon Nanotube: An Overview of Synthesis, Properties, Functionalization, Characterization, and the Application. *Materials Science and Engineering*: *B*, **268**, 115095-116122. https://doi.org/10.1016/j.mseb.2021.115095

[9] Nguyen Thi, T.B., Ata, S., Morimoto, T., Yamada, T., Okazaki, T. and Hata, K.

(2021) Tailoring the Electrically Conductive Network of Injection-Molded Polymer-Carbon Nanotube Composite at Low Filler Content. *Materials Today: Proceedings*, **40**, 5-8. https://doi.org/10.1016/j.matpr.2020.02.137

[10] Khan, T., Irfan, M.S., Ali, M., Dong, Y., Ramakrishna, S. and Umer, R. (2021) Insights to Low Electrical Percolation Thresholds of Carbon-Based Polypropylene Nanocomposites. *Carbon*, **176**, 602-631. https://doi.org/10.1016/j.carbon.2021.01.158

[11] Gorrasi, G., Milone, C., Piperopoulos, E., Lanza, M. and Sorrentino, A. (2013) Hybrid Clay Mineral-Carbon Nanotube-PLA Nanocomposite Films. Preparation and Photodegradation Effect on Their Mechanical, Thermal and Electrical Properties. *Applied Clay Science*, **71**, 49-54. https://doi.org/10.1016/j.clay.2012.11.004

[12] Quan, H., Zhang, S.-J., Qiao, J.-L. and Zhang, L.-Y. (2012) The Electrical Properties and Crystallization of Stereocomplex Poly(lactic acid) Filled with Carbon Nanotubes. *Polymer*, **53**, 4547-4552. https://doi.org/10.1016/j.polymer.2012.07.061

[13] Mandal, A. and Nandi, A.K. (2013) Ionic Liquid Integrated Multiwalled Carbon Nanotube in a Poly(vinylidene fluoride) Matrix: Formation of a Piezoelectric β-Polymorph with Significant Reinforcement and Conductivity Improvement. *ACS Applied Materials & Interfaces*, **5**, 747-760. https://doi.org/10.1021/am302275b

[14] Amirian, M., Nabipour Chakoli, A., Cai, W. and Sui, J. (2013) Effect of Functionalized Multiwalled Carbon Nanotubes on Thermal Stability of Poly(L-Lactide) Biodegradable Polymer. *Scientia Iranica*, **20**, 1023-1027.

[15] He, X., Zhang, F., Wang, R. and Liu, W. (2007) Preparation of a Carbon Nanotube/Carbon Fiber Multi-Scale Reinforcement by Grafting Multi-Walled Carbon Nanotubes onto the Fibers. *Carbon*, **45**, 2559-2563. https://doi.org/10.1016/j.carbon.2007.08.018

[16] Liu, P. (2005) Modifications of Carbon Nanotubes with Polymers. *European Polymer Journal*, **41**, 2693-2703. https://doi.org/10.1016/j.eurpolymj.2005.05.017

[17] Laredo, E., Grimau, M., Bello, A., Wu, D.F., Zhang, Y.S. and Lin, D.P. (2010) AC Conductivity of Selectively Located Carbon Nanotubes in Poly(ε-caprolactone)/Polylactide Blend Nanocomposites. *Biomacromolecules*, **11**, 1339-1347. https://doi.org/10.1021/bm100135n

[18] Bouchard, J., Cayla, A., Devaux, E. and Campagne, C. (2013) Electrical and Thermal Conductivities of Multiwalled Carbon Nanotubes-Reinforced High Performance Polymer Nanocomposites. *Composites Science and Technology*, **86**, 177-184. https://doi.org/10.1016/j.compscitech.2013.07.017

[19] Shrivastava, N.K. and Khatua, B.B. (2011) Development of Electrical Conductivity with Minimum Possible Percolation Threshold in Multi-Wall Carbon Nanotube/Polystyrene Composites. *Carbon*, **49**, 4571-4579. https://doi.org/10.1016/j.carbon.2011.06.070

[20] Yoon, J.T., Lee, S.C. and Jeong, Y.G. (2010) Effects of Grafted Chain Length on Mechanical and Electrical Properties of Nanocomposites Containing Polylactide-Grafted Carbon Nanotubes. *Composites Science and Technology*, **70**, 776-782. https://doi.org/10.1016/j.compscitech.2010.01.011

[21] Seligra, P.G., Nuevo, F., Lamanna, M. and Famá, L. (2013) Covalent Grafting of Carbon Nanotubes to PLA in Order to Improve Compatibility. *Composites Part B: Engineering*, **46**, 61-68. https://doi.org/10.1016/j.compositesb.2012.10.013

[22] Wang, Q., Han, Y., Wang, Y., Qin, Y. and Guo, Z.-X. (2008) Effect of Surfactant Structure on the Stability of Carbon Nanotubes in Aqueous Solution. *The Journal of Physical Chemistry B*, **112**, 7227-7233. https://doi.org/10.1021/jp711816c

[23] Tang, Q.-Y., Chen, J., Chan, Y.C. and Chung, C.Y. (2010) Effect of Carbon Nanotubes and Their Dispersion on Thermal Curing of Polyimide Precursors. *Polymer Degradation and Stability*, **95**, 1672-1678. https://doi.org/10.1016/j.polymdegradstab.2010.05.023

[24] Pegel, S., Pötschke, P., Petzold, G., Alig, I., Dudkin, S.M. and Lellinger, D. (2008) Dispersion, Agglomeration, and Network Formation of Multiwalled Carbon Nanotubes in Polycarbonate Melts. *Polymer*, **49**, 974-984. https://doi.org/10.1016/j.polymer.2007.12.024

[25] Alig, I., Pötschke, P., Lellinger, D., Skipa, T., Pegel, S., Kasaliwal, G.R. and Villmow, T. (2012) Establishment, Morphology and Properties of Carbon Nanotube Networks in Polymer Melts. *Polymer*, **53**, 4-28. https://doi.org/10.1016/j.polymer.2011.10.063

[26] Gong, X.Y., Liu, J., Baskaran, S., Voise, R.D. and Young, J.S. (2000) Surfactant-Assisted Processing of Carbon Nanotube/Polymer Composites. *Chemistry of Materials*, **12**, 1049-1052. https://doi.org/10.1021/cm9906396

[27] Kilbride, B.E., Coleman, J.N., Fraysse, J., Fournet, P., Cadek, M., Drury, A., Hutzler, S., Roth, S. and Blau, W.J. (2002) Experimental Observation of Scaling Laws for Alternating Current and Direct Current Conductivity in Polymer-Carbon Nanotube Composite Thin Films. *Journal of Applied Physics*, **92**, 4024-4030. https://doi.org/10.1063/1.1506397

[28] Bauhofer, W. and Kovacs, J.Z. (2009) A Review and Analysis of Electrical Percolation in Carbon Nanotube Polymer Composites. *Composites Science and Technology*, **69**, 1486-1498. https://doi.org/10.1016/j.compscitech.2008.06.018

[29] Xu, Y.H., Li, Q.F., Sun, D., Zhang, W.J. and Chen, G.X. (2012) A Strategy To Functionalize the Carbon Nanotubes and the Nanocomposites Based on Poly(l-lactide). *Industrial & Engineering Chemistry Research*, **51**, 13648-13654. https://doi.org/10.1021/ie300989w